

## Self-consistent electron lifetimes for electron-phonon scattering

Jae-Mo Lihm<sup>1,2,3,\*</sup>, Samuel Poncé<sup>4,5,†</sup> and Cheol-Hwan Park<sup>1,2,3,‡</sup>

<sup>1</sup>Department of Physics and Astronomy, Seoul National University, Seoul 08826, Korea

<sup>2</sup>Center for Correlated Electron Systems, Institute for Basic Science, Seoul 08826, Korea

<sup>3</sup>Center for Theoretical Physics, Seoul National University, Seoul 08826, Korea

<sup>4</sup>European Theoretical Spectroscopy Facility, Institute of Condensed Matter and Nanosciences, Université catholique de Louvain, Chemin des Étoiles 8, B-1348 Louvain-la-Neuve, Belgium

<sup>5</sup>WEL Research Institute, Avenue Pasteur, 6, 1300 Wavre, Belgique



(Received 17 January 2024; accepted 23 August 2024; published 11 September 2024)

Acoustic phonons in piezoelectric materials strongly couple to electrons through a macroscopic electric field. We show that this coupling leads to a momentum-dependent divergence of the Fan-Migdal electron linewidth. We then develop a self-consistent theory for calculating electron linewidths, which not only removes this piezoelectric divergence but also considerably modifies the linewidth in nonpiezoelectric, polar materials. Our predictions await immediate experimental confirmation, and this self-consistent method should be broadly used in interpreting various experiments on the electronic properties of real materials.

DOI: [10.1103/PhysRevB.110.L121106](https://doi.org/10.1103/PhysRevB.110.L121106)

Piezoelectricity, the change in polarization in response to a mechanical strain, is a common phenomenon allowed in 20 out of 21 noncentrosymmetric point groups [1]. It induces a coupling between electrons and acoustic phonons mediated by a long-range electric field [2]. In recent years, there has been a significant increase in the interest in the calculation of piezoelectric electron-phonon coupling (EPC) and its effect on electronic properties [3–15]. The combination of Wannier interpolation [16–19] with analytically calculated long-range Fröhlich and piezoelectric EPC in terms of dipole and quadrupole moments [7–15,20] enables a fully *ab initio* study of the effects of EPC on the spectral and transport properties of piezoelectric materials.

Interestingly, in the presence of piezoelectric EPC, the electron linewidth diverges when calculated from the perturbative Fan-Migdal formula [21], the current standard for calculating carrier linewidths from first principles [22,23]. This divergence should occur when using a vanishing broadening [24], an adaptive broadening [12,15,25], or even the tetrahedron integration method [9,26]. Even though this divergence implies that calculations of the linewidths cannot be converged, it has not been considered in first-principles calculations of piezoelectric materials [7–11,14,15]. Calculations with a finite broadening would lead to results that depend sensitively on artificial computational parameters [24].

In this work, we study the limitation of the one-shot calculation of electron lifetimes in piezoelectric materials and prove that a self-consistent broadening of the electrons is required. First, we find that the piezoelectric divergence depends on the electron wave vector and confirm this finding with first-principles calculations. Then, we develop a formalism

based on the quasiparticle approximation to self-consistently calculate the linewidths and apply it to study the EPC in cubic boron nitride (c-BN), Si, NaCl, and PbTe. We find that self-consistency dominates the regularization of piezoelectric EPC for weak to intermediate doping and quantitatively affects the results even at higher doping. Furthermore, we find that self-consistency also affects the scattering due to polar optical phonons in both piezoelectric and nonpiezoelectric materials, leading to a complex dependence of the linewidths on the electron energy, temperature, and doping. Our prediction can be directly confirmed by angle-resolved photoemission experiments [27–29]. The self-consistent linewidths should be broadly applied to the computations of transport, optical, and spectroscopic properties.

The Fan-Migdal formula for the phonon-induced electron linewidth at band  $n$  and wave vector  $\mathbf{k}$  reads [23,30,31]

$$\begin{aligned} \gamma_{nk} = & \frac{2\pi}{\hbar} \sum_{mv} \int \frac{d\mathbf{q}}{\Omega^{\text{BZ}}} |g_{m\nu}(\mathbf{k}, \mathbf{q})|^2 \\ & \times \sum_{\pm} \{ [n_{\mathbf{q}\nu} + f^{\pm}(\varepsilon_{m\mathbf{k}+\mathbf{q}})] \delta(\varepsilon_{n\mathbf{k}} - \varepsilon_{m\mathbf{k}+\mathbf{q}} \pm \hbar\omega_{\mathbf{q}\nu}) \}, \end{aligned} \quad (1)$$

where  $\Omega^{\text{BZ}}$  is the volume of the Brillouin zone,  $n_{\mathbf{q}\nu}$  the phonon occupation at wave vector  $\mathbf{q}$  and mode  $\nu$ ,  $f^{\pm}(\varepsilon_{m\mathbf{k}+\mathbf{q}})$  is the electron occupation,  $f^{-}(\varepsilon_{m\mathbf{k}+\mathbf{q}}) = 1 - f^{+}(\varepsilon_{m\mathbf{k}+\mathbf{q}})$ ,  $g_{m\nu}(\mathbf{k}, \mathbf{q})$  the electron-phonon matrix element, and  $\varepsilon_{n\mathbf{k}}$  and  $\hbar\omega_{\mathbf{q}\nu}$  the electron and phonon energies, respectively. The linewidth  $\gamma_{nk}$  is the inverse of the carrier lifetime  $\tau_{nk}$  and twice the imaginary part of the electron self-energy  $\Sigma_{nk}$ ,  $\gamma_{nk} = 1/\tau_{nk} = 2|\text{Im} \Sigma_{nk}|/\hbar$  [32].

To analyze the linewidths due to piezoelectric EPC, we start with a three-dimensional isotropic long-wavelength model:  $\varepsilon_{\mathbf{k}} = \frac{\hbar^2 k^2}{2m}$ ,  $\omega_{\mathbf{q}} = qv^{\text{ph}}$ , where  $m$  is the electron effective mass and  $v^{\text{ph}}$  the phonon velocity. We set  $\varepsilon_{\mathbf{k}} = 0$  at

\*Contact author: jaemo.lihm@gmail.com

†Contact author: samuel.ponce@uclouvain.be

‡Contact author: cheolhwan@snu.ac.kr

the conduction-band minimum (CBM) throughout this paper. We consider the piezoelectric EPC with longitudinal acoustic phonons [21], which originates from the long-range Coulomb interaction and is discontinuous at  $\mathbf{q} = 0$ .

Let us regularize the delta function in Eq. (1) with a Lorentzian

$$\delta_\eta(\varepsilon) = \frac{1}{\pi} \frac{\eta/2}{\varepsilon^2 + (\eta/2)^2}. \quad (2)$$

Using other regularization functions such as Gaussians does not alter the conclusions qualitatively. Evaluating the integral in Eq. (1) yields

$$\gamma_k \propto \begin{cases} \frac{1}{k} \ln \frac{\varepsilon_k}{\eta} & \text{if } v_k^{\text{el}} > v^{\text{ph}} (k > mv^{\text{ph}}/\hbar), \\ \frac{1}{k} \ln \frac{v^{\text{ph}} + v_k^{\text{el}}}{v^{\text{ph}} - v_k^{\text{el}}} & \text{if } v_k^{\text{el}} < v^{\text{ph}} (k < mv^{\text{ph}}/\hbar), \end{cases} \quad (3)$$

where  $v_k^{\text{el}} = \hbar k/m$  is the band velocity of the electron at wave vector  $\mathbf{k}$  (see Eqs. (S15) and (S26) of the SM [33]).

For the first case where  $v_k^{\text{el}} > v^{\text{ph}}$ , the linewidth diverges logarithmically in the zero-broadening limit  $\eta \rightarrow 0^+$ . A similar logarithmic divergence has been found using an artificial infrared cutoff of phonon wave vector  $q$  instead of the finite broadening (see Sec. 3.6 of Ref. [21]). In the second case with  $v_k^{\text{el}} < v^{\text{ph}}$ , the linewidth converges to a finite value. Due to the  $1/k$  prefactor in Eq. (3), for a sufficiently small  $\eta$ , the linewidth is peaked around  $k = mv^{\text{ph}}/\hbar$  where  $v_k^{\text{el}} = v^{\text{ph}}$ . This dichotomy of the Brillouin zone into a divergent and convergent region is an important finding of this work.

This logarithmic divergence originates from the absorption and emission of acoustic phonons with an infinitesimal wave vector. Figures 1(a) and 1(b) illustrate the dispersion that disallows and allows the infinitesimal-wave-vector scattering, respectively; only the latter leads to the divergence. The criterion for divergence can be generalized to an arbitrary three-dimensional dispersion. To have infinitesimal-wave-vector scattering, one needs a direction  $\hat{q}$  where the electron and acoustic phonon velocities are identical:

$$\mathbf{v}_{nk}^{\text{el}} \cdot \hat{q} = \mathbf{v}_{0\nu}^{\text{ph}} \cdot \hat{q} \text{ for some } \hat{q} \text{ and } \nu \in 1, 2, 3. \quad (4)$$

We confirmed this behavior by performing *ab initio* calculations whose details are provided in the SM [33]. Figure 1(c) shows the *ab initio* linewidths for the conduction-band states of c-BN. We performed an ultradense nonuniform sampling near  $\Gamma$ , with a density reaching that of a  $(5 \times 10^7)^3$  homogeneous  $\mathbf{q}$ -point grid. The CBM is located at  $\mathbf{k}_X = \frac{2\pi}{a}\hat{z}$ , where  $a$  is the cubic lattice parameter. For a  $\mathbf{k}$  point on the  $\Gamma X$  line, the condition Eq. (4) for  $\hat{q} \parallel \mathbf{k}_X$  reads

$$|(\mathbf{k} - \mathbf{k}_X) \cdot \hat{z}| = \frac{m_z v_z^{\text{ph}}}{\hbar} = \frac{m_z}{\hbar} \sqrt{\frac{C_{44}}{\rho}} = 0.0080 \text{ \AA}^{-1}, \quad (5)$$

where  $C_{44}$  is the shear modulus and  $\rho$  the mass density. By scanning all  $\hat{q}$  directions, we find a lower bound of  $|k_z - \frac{2\pi}{a}| > 0.0078 \text{ \AA}^{-1} = 0.0045 \frac{2\pi}{a}$  for the presence of the logarithmic divergence where Eq. (4) is satisfied at  $\hat{q} = (\sin 0.1\pi, 0, \cos 0.1\pi)$  due to a small anisotropy in the dispersion. Figure 1(c) verifies this criterion, as the linewidths at  $|\mathbf{k} - \mathbf{k}_X| \leq 0.004|\mathbf{k}_X|$  converge to a finite value in the  $\eta \rightarrow 0^+$  limit, while those at  $|\mathbf{k} - \mathbf{k}_X| \geq 0.005|\mathbf{k}_X|$  diverge logarithmically in  $\eta$ .

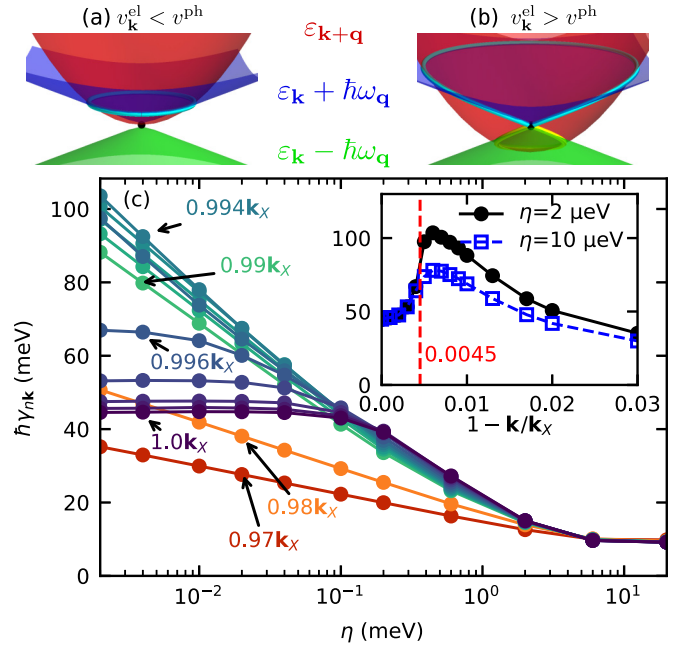


FIG. 1. (a), (b) Dispersion of electrons and phonons. We show two-dimensional dispersions for a simpler visualization. The  $\mathbf{q}$  points where energy-conserving phonon absorption or emission is allowed is indicated by cyan and yellow, respectively. (c) Linewidths at the conduction band of intrinsic c-BN at  $T = 300$  K as a function of broadening for  $\mathbf{k}$  points along the  $\Gamma X$  line. Inset: linewidths as a function of wave vectors for two broadening values. The vertical red dashed line indicates the onset of the divergence.

Since this divergence is logarithmic, it is easy to misinterpret it as a convergence, which explains why the divergence was not reported in any of the previous *ab initio* calculations. For a given broadening  $\eta$ , capturing the correct momentum dependence of the linewidths requires resolving phonon modes with energy as low as  $\eta$  and wave vectors as small as  $\eta/\hbar v^{\text{ph}}$ . For c-BN, one would need a  $\mathbf{q}$ -point density of  $1/6000^3$ , albeit only at the zone center, to get the correct momentum dependence at  $\eta = 0.2$  meV, where the divergence becomes barely noticeable [Fig. 1(c)]. Such a grid is more than three orders of magnitude denser than the ones commonly used in *ab initio* calculations [23,62]. We emphasize that this divergence is an artifact of the zero-broadening formula and does not reflect experimental observations.

We remark that since the piezoelectric scattering is dominated by small- $q$  phonons, it conserves the electron momentum and therefore does not contribute to the electrical resistivity when calculated with the full Boltzmann transport equation. Hence, the mobility of c-BN calculated using the Boltzmann transport equation converges rapidly with the density of the  $\mathbf{q}$  points [12].

We now study the role of self-consistent broadening in regularizing this divergence. Since the linewidths broaden the electronic spectral function, the energy-conserving delta function in Eq. (1) should be broadened accordingly. By evaluating the Fan-Migdal self-energy under the quasiparticle approximation and taking the imaginary part of the self-energy at the quasiparticle energy as the linewidth, we derive a

self-consistent formula for the linewidth (see Sec. S2 [33]):

$$\begin{aligned} \gamma_{nk} &= \frac{2\pi}{\hbar} \sum_{mv} \int \frac{d\mathbf{q}}{\Omega_{\text{BZ}}} |g_{mv}(\mathbf{k}, \mathbf{q})|^2 \\ &\times \sum_{\pm} \{ [n_{\mathbf{q}_v} + f^{\pm}(\varepsilon_{n\mathbf{k}} \pm \hbar\omega_{\mathbf{q}_v})] \\ &\times \delta_{\hbar\gamma_{m\mathbf{k}+\mathbf{q}}}(\varepsilon_{n\mathbf{k}} - \varepsilon_{m\mathbf{k}+\mathbf{q}} \pm \hbar\omega_{\mathbf{q}_v}) \}. \end{aligned} \quad (6)$$

The self-consistent broadening  $\gamma_{nk}$  is calculated for each temperature.

There are two key differences compared to the non-self-consistent formula, Eq. (1). First, the delta function is replaced with a Lorentzian [Eq. (2)] with a self-consistent width  $\hbar\gamma_{m\mathbf{k}+\mathbf{q}}$ . Second, the occupation function  $f^{\pm}(\varepsilon_{n\mathbf{k}} \pm \hbar\omega_{\mathbf{q}_v})$  is used instead of  $f^{\pm}(\varepsilon_{m\mathbf{k}+\mathbf{q}})$ . The two occupations can be used interchangeably in the limit  $\hbar\gamma_{m\mathbf{k}+\mathbf{q}} \ll k_B T$  because of the energy-conserving delta function. Otherwise, the two formulas give different results. For example, at  $T = 0$ , only the correct formula using  $f^{\pm}(\varepsilon_{n\mathbf{k}} \pm \hbar\omega_{\mathbf{q}_v})$  gives a vanishing linewidth at the Fermi surface. The approximation  $f^{\pm}(\varepsilon_{n\mathbf{k}} \pm \hbar\omega_{\mathbf{q}_v}) \approx f^{\pm}(\varepsilon_{m\mathbf{k}+\mathbf{q}})$  has been adopted in Ref. [63] for a self-consistent calculation of electron lifetimes.

The renormalization of the phonon energies and spectral function may also be similarly included, by modifying the phonon frequency and occupation factors in Eq. (6). However, in the low- to intermediate-doping regime, which we focus on in this work, the adiabatic density-functional perturbation theory is expected to work well for the phonons [22], and the phonon renormalization can be viewed as a secondary effect. In fact, in the intrinsic, undoped case, the phonon dispersion does not get renormalized, while the electron spectral functions are still strongly renormalized.

Another mechanism that regularizes the logarithmic divergence is the free-carrier screening [21]. In doped semiconductors, free carriers screen the long-range Coulomb interaction to make it finite ranged. This screening is important for longitudinal optical (LO) phonons [64–67] and ionized impurity potentials [68,69]. For the piezoelectric EPC, the screening regularizes the  $\mathcal{O}(q^0)$  discontinuity of the EPC at  $q = 0$  to a smoothly decaying function with a characteristic wave vector given by the Thomas-Fermi wave vector. In metals, free carriers will completely screen the piezoelectric EPC. However, when the doping is not too heavy, the piezoelectric EPC will still make a large contribution to the linewidth. In this case, self-consistency plays an important role.

Figure 2 compares the linewidths at two different doping levels. The doping is included via the change in the electron occupation factor and the free-carrier screening of EPC [Eq. (S94)], while the electron and phonon dispersions are taken from calculations on the undoped system. We identify two distinct regimes. For a low doping  $n \leq 10^{16} \text{ cm}^{-3}$ , the self-consistent linewidths display a monotonic energy dependence in the shown energy range. In contrast, the fixed-broadening linewidths display a sharp peak at an energy below 5 meV, which originates from the piezoelectric divergence regularized by the free-carrier screening. In this regime, self-consistency plays a dominant role in regularizing the piezoelectric scattering. For a higher doping  $n \geq 10^{17} \text{ cm}^{-3}$ , the low-energy peak disappears but quantitative differences

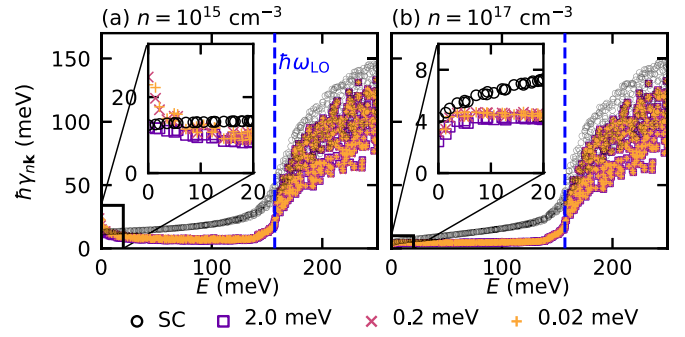


FIG. 2. Electron linewidth of c-BN at  $T = 300 \text{ K}$  at different doping levels  $n$ . Black circles show the self-consistent (SC) linewidths while the others show those computed at a fixed broadening. Blue vertical dashed lines indicate the LO phonon frequency.

between the fixed-broadening and self-consistent linewidths remain, especially at energies  $\varepsilon_{n\mathbf{k}} \lesssim \hbar\omega_{\text{LO}}$ . These differences are due to the LO phonon scattering, which is heavily broadened due to a large linewidth of the electrons above the LO phonon energy. We note that free-carrier screening of the LO phonons ( $\omega \approx 160 \text{ meV}$ ) is negligible at the considered carrier densities ( $n \leq 10^{18} \text{ cm}^{-3}$ ) since the LO phonon frequency is much higher than the plasma frequency ( $\omega \lesssim 25 \text{ meV}$ ) [64].

This analysis leads to our main finding that self-consistency may qualitatively change the energy dependence of electron linewidths. To demonstrate that such a strong effect is a generic phenomenon that does not require piezoelectricity, we apply our theory of self-consistent linewidths to three nonpiezoelectric materials, Si, PbTe, and NaCl. We compare the self-consistent calculation with fixed-broadening calculations with three different broadenings, chosen from the smallest self-consistent linewidth of each material. Figures 3(a)–3(c) show that while the linewidths of Si are affected only slightly by broadening parameters and self-consistency, those of PbTe and NaCl vary significantly. Compared to the  $\eta = 0.6 \text{ meV}$  results, self-consistency

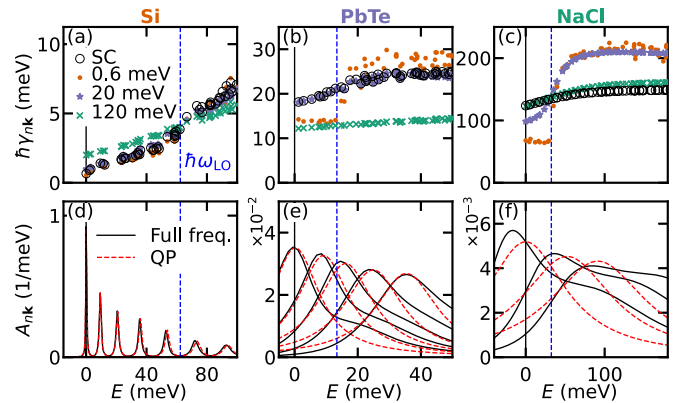


FIG. 3. (a)–(c) Linewidths at the conduction band of Si, PbTe, and NaCl at  $T = 300 \text{ K}$  and  $n = 10^{13} \text{ cm}^{-3}$  with self-consistent lifetime (empty circle) and fixed broadening (filled symbols). (d)–(f) Full-frequency and quasiparticle (QP) spectral functions along the  $\Gamma X$  line for  $|\mathbf{k}|/|\mathbf{k}_x|$  values (d) 0.82, 0.86, 0.88, 0.9, 0.92, 0.94, and 0.96 for Si; (e) 1, 0.97, 0.96, 0.95, and 0.94 for PbTe; and (f) 0, 0.06, and 0.08 for NaCl, from left to right.

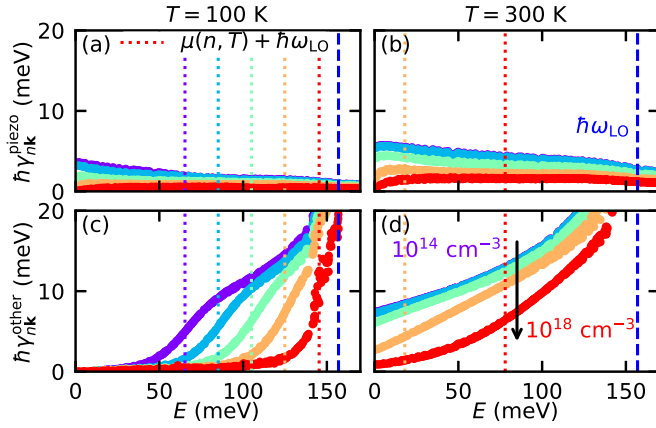


FIG. 4. (a), (b) Piezoelectric and (c), (d) other contributions to the linewidth of c-BN at varying doping and using self-consistent broadening. Consecutive curves show results for systems with ten times different doping levels  $n$ , going from violet ( $10^{14} \text{ cm}^{-3}$ ) to red ( $10^{18} \text{ cm}^{-3}$ ). The values of  $\mu(n, T) + \omega_{LO}$ , where  $\mu$  is the chemical potential, are indicated by vertical dotted lines in color.

substantially smoothens the sharp rise of electron linewidths at the LO-phonon energy. We also find that while fine-tuning can yield fixed-broadening results comparable to the self-consistent calculation, the value of the “optimal” broadening parameter is highly material dependent, spanning over two orders of magnitude, and cannot be determined *a priori*. The deviations of over several tens of meV’s are well above the current resolution for angle-resolved photoemission spectroscopy and can be directly confirmed from experiments [27–29].

Figures 3(d)–3(f) show the spectral functions obtained from a one-shot calculation of the frequency-dependent self-energy using the converged self-consistent broadening (see Sec. S3 for details [33]). For Si and PbTe, the two spectral functions agree very well, especially in the low-energy part, providing a strong validation of the quasiparticle approximation. We also find a similar agreement for c-BN (Fig. S4). For NaCl, where the EPC is the strongest, the deviation is larger, but the quasiparticle approximation still captures the width of the spectral function.

The doping dependence of the linewidth has two major contributions, the piezoelectric scattering from acoustic phonons and the scattering from the LO phonons. To understand their respective roles, we use a long-wavelength model that solely contains the acoustic phonons and their piezoelectric EPC with parameters computed from the piezoelectric and elastic tensors (see Sec. S4). We write the total linewidth as the sum of the piezoelectric contribution and the remainder, i.e.,

$$\gamma_{nk} = \gamma_{nk}^{\text{piezo}} + \gamma_{nk}^{\text{other}}. \quad (7)$$

Figures 4(a) and 4(b) show that  $\gamma_{nk}^{\text{piezo}}$  decreases with doping due to the free-carrier screening of the piezoelectric EPC. In contrast, since the screening is ineffective for the LO phonon, and the doping dependence of  $\gamma_{nk}^{\text{other}}$  in Figs. 4(c) and 4(d) originates from the change in the chemical potential. At  $k_B T \ll \hbar\omega_{LO}$ , where the LO-phonon occupation is negligible, the linewidth is almost zero for states with energy

below  $\mu + \omega_{LO}$ . This behavior is a consequence of the general principle that at  $T = 0$  the emission of a phonon with energy  $\hbar\omega_{LO}$  is not allowed for states with energy inside the window  $[\mu - \hbar\omega_{LO}, \mu + \hbar\omega_{LO}]$ , since for an electron with energy  $\varepsilon_{nk} < \mu + \hbar\omega_{LO}$  the final state has energy  $\varepsilon_{nk} - \hbar\omega_{LO} < \mu$  and is fully occupied, forbidding the transition. At finite temperatures, this feature is broadened, resulting in a smooth increase centered at  $\mu + \hbar\omega_{LO}$ , as shown in Figs. 4(c) and 4(d). If a fixed broadening is used (Fig. S2), or if  $f(\varepsilon_{nk} \pm \hbar\omega_{LO})$  in Eq. (6) is approximated by  $f(\varepsilon_{m\mathbf{k}+\mathbf{q}})$  (Fig. S4), this feature disappears.

Self-consistency in the EPC can affect many electronic properties such as the broadening of the electron spectral function measured from angle-resolved photoemission spectroscopy [70–72], optical absorption spectra [73–75], phonon-mediated superconductivity [76–78], and phonon-limited transport [23,24,79]. Incorporating self-consistency in the study of these quantities and reexamining *ab initio* calculations would be desirable. The effect of the self-consistent linewidth on the ionized impurity linewidths [68,69] could also be studied. The effect of piezoelectric EPC on low-dimensional materials, for which one of the acoustic phonon branches displays a quadratic dispersion [80,81], is another interesting venue for future research. Our work also forms the foundation for going beyond the simple perturbative treatment of EPC in first-principles studies. A straightforward generalization to full spectral self-consistency [82] could capture the reduction in the quasiparticle weight and the appearance of satellite peaks [64,65,83].

In conclusion, we show that the calculation of the electron lifetime for piezoelectric materials in the zero-broadening limit breaks down and needs to be replaced with a self-consistent method. We implement a self-consistent equation for the electron linewidth using the quasiparticle approximation and apply it to c-BN, Si, PbTe, and NaCl. We find that self-consistency plays a central role in regularizing the piezoelectric EPC for a wide range of experimentally relevant doping and strongly affects the doping dependence of the LO-phonon scattering. Therefore, our theory should be broadly applied to various experiments on electronic properties. Finally, our predictions on the energy-dependent electron linewidths, which are qualitatively different from conventional calculations, await immediate experimental confirmation.

J.-M.L. and C.-H.P. were supported by the Creative-Pioneering Research Program through Seoul National University, Korean NRF No. 2023R1A2C1007297, and the Institute for Basic Science (No. IBSR009-D1). S.P. acknowledges support from the Fonds de la Recherche Scientifique de Belgique (FRS-FNRS) and by the Walloon Region in the strategic axe FRFS-WEL-T. Computational resources have been provided by KISTI (KSC-2022-CRE-0407), the PRACE award granting access to MareNostrum4 at Barcelona Supercomputing Center (BSC), Spain and Discoverer in SofiaTech, Bulgaria (OptoSpin Project ID 2020225411), the Consortium des Équipements de Calcul Intensif (CÉCI), funded by the FRS-FNRS under Grant No. 2.5020.11, and by the Walloon Region, as well as computational resources awarded on the Belgian share of the EuroHPC LUMI supercomputer.

- [1] P. S. Halasyamani and K. R. Poeppelmeier, Noncentrosymmetric oxides, *Chem. Mater.* **10**, 2753 (1998).
- [2] R. M. Martin, Piezoelectricity, *Phys. Rev. B* **5**, 1607 (1972).
- [3] D. Vanderbilt, Berry-phase theory of proper piezoelectric response, *J. Phys. Chem. Solids* **61**, 147 (2000).
- [4] D. R. Hamann, X. Wu, K. M. Rabe, and D. Vanderbilt, Metric tensor formulation of strain in density-functional perturbation theory, *Phys. Rev. B* **71**, 035117 (2005).
- [5] M. Stengel, Flexoelectricity from density-functional perturbation theory, *Phys. Rev. B* **88**, 174106 (2013).
- [6] M. Royo and M. Stengel, First-principles theory of spatial dispersion: Dynamical quadrupoles and flexoelectricity, *Phys. Rev. X* **9**, 021050 (2019).
- [7] T.-H. Liu, J. Zhou, B. Liao, D. J. Singh, and G. Chen, First-principles mode-by-mode analysis for electron-phonon scattering channels and mean free path spectra in GaAs, *Phys. Rev. B* **95**, 075206 (2017).
- [8] G. Brunin, H. P. C. Miranda, M. Giantomassi, M. Royo, M. Stengel, M. J. Verstraete, X. Gonze, G.-M. Rignanese, and G. Hautier, Electron-phonon beyond Fröhlich: Dynamical quadrupoles in polar and covalent solids, *Phys. Rev. Lett.* **125**, 136601 (2020).
- [9] G. Brunin, H. P. C. Miranda, M. Giantomassi, M. Royo, M. Stengel, M. J. Verstraete, X. Gonze, G.-M. Rignanese, and G. Hautier, Phonon-limited electron mobility in Si, GaAs, and GaP with exact treatment of dynamical quadrupoles, *Phys. Rev. B* **102**, 094308 (2020).
- [10] V. A. Jhalani, J.-J. Zhou, J. Park, C. E. Dreyer, and M. Bernardi, Piezoelectric electron-phonon interaction from *ab initio* dynamical quadrupoles: Impact on charge transport in wurtzite GaN, *Phys. Rev. Lett.* **125**, 136602 (2020).
- [11] J. Park, J.-J. Zhou, V. A. Jhalani, C. E. Dreyer, and M. Bernardi, Long-range quadrupole electron-phonon interaction from first principles, *Phys. Rev. B* **102**, 125203 (2020).
- [12] S. Ponc e, F. Macheda, E. R. Margine, N. Marzari, N. Bonini, and F. Giustino, First-principles predictions of Hall and drift mobilities in semiconductors, *Phys. Rev. Res.* **3**, 043022 (2021).
- [13] A. M. Ganose, J. Park, A. Faghaninia, R. Woods-Robinson, K. A. Persson, and A. Jain, Efficient calculation of carrier scattering rates from first principles, *Nat. Commun.* **12**, 2222 (2021).
- [14] S. Ponc e, M. Royo, M. Gibertini, N. Marzari, and M. Stengel, Accurate prediction of Hall mobilities in two-dimensional materials through gauge-covariant quadrupolar contributions, *Phys. Rev. Lett.* **130**, 166301 (2023).
- [15] S. Ponc e, M. Royo, M. Stengel, N. Marzari, and M. Gibertini, Long-range electrostatic contribution to electron-phonon couplings and mobilities of two-dimensional and bulk materials, *Phys. Rev. B* **107**, 155424 (2023).
- [16] N. Marzari and D. Vanderbilt, Maximally-localized generalized Wannier functions for composite energy bands, *Phys. Rev. B* **56**, 12847 (1997).
- [17] I. Souza, N. Marzari, and D. Vanderbilt, Maximally localized Wannier functions for entangled energy bands, *Phys. Rev. B* **65**, 035109 (2001).
- [18] F. Giustino, M. L. Cohen, and S. G. Louie, Electron-phonon interaction using Wannier functions, *Phys. Rev. B* **76**, 165108 (2007).
- [19] N. Marzari, A. A. Mostofi, J. R. Yates, I. Souza, and D. Vanderbilt, Maximally localized Wannier functions: Theory and applications, *Rev. Mod. Phys.* **84**, 1419 (2012).
- [20] C. Verdi and F. Giustino, Fr ohlich electron-phonon vertex from first principles, *Phys. Rev. Lett.* **115**, 176401 (2015).
- [21] B. K. Ridley, *Quantum Processes in Semiconductors* (Oxford University Press, Oxford, 1982).
- [22] F. Giustino, Electron-phonon interactions from first principles, *Rev. Mod. Phys.* **89**, 015003 (2017).
- [23] S. Ponc e, W. Li, S. Reichardt, and F. Giustino, First-principles calculations of charge carrier mobility and conductivity in bulk semiconductors and two-dimensional materials, *Rep. Prog. Phys.* **83**, 036501 (2020).
- [24] S. Ponc e, E. R. Margine, and F. Giustino, Towards predictive many-body calculations of phonon-limited carrier mobilities in semiconductors, *Phys. Rev. B* **97**, 121201 (2018).
- [25] W. Li, J. Carrete, N. A. Katcho, and N. Mingo, ShengBTE: A solver of the Boltzmann transport equation for phonons, *Comput. Phys. Commun.* **185**, 1747 (2014).
- [26] P. E. Bl ochl, O. Jepsen, and O. K. Andersen, Improved tetrahedron method for Brillouin-zone integrations, *Phys. Rev. B* **49**, 16223 (1994).
- [27] A. Bostwick, T. Ohta, T. Seyller, K. Horn, and E. Rotenberg, Quasiparticle dynamics in graphene, *Nat. Phys.* **3**, 36 (2007).
- [28] C.-H. Park, F. Giustino, M. L. Cohen, and S. G. Louie, Velocity renormalization and carrier lifetime in graphene from the electron-phonon interaction, *Phys. Rev. Lett.* **99**, 086804 (2007).
- [29] C.-H. Park, F. Giustino, C. D. Spataru, M. L. Cohen, and S. G. Louie, First-principles study of electron linewidths in graphene, *Phys. Rev. Lett.* **102**, 076803 (2009).
- [30] G. D. Mahan, *Many-Particle Physics*, 3rd ed. (Kluwer Academic/Plenum Publishers, New York, 2000).
- [31] G. Grimvall, *The Electron-Phonon Interaction in Metals* (North-Holland, Amsterdam, 1981).
- [32] S. Ponc e, E. Margine, C. Verdi, and F. Giustino, EPW: Electron-phonon coupling, transport and superconducting properties using maximally localized Wannier functions, *Comput. Phys. Commun.* **209**, 116 (2016).
- [33] See Supplemental Material at <http://link.aps.org/supplemental/10.1103/PhysRevB.110.L121106> for the derivation of the self-consistent theory and computational details, which includes Refs. [34–61].
- [34] G. Arlt and P. Quadflieg, Piezoelectricity in III–V compounds with a phenomenological analysis of the piezoelectric effect, *Physica Status Solidi (b)* **25**, 323 (1968).
- [35] G. Stefanucci and R. Van Leeuwen, *Nonequilibrium Many-Body Theory of Quantum Systems: A Modern Introduction* (Cambridge University Press, Cambridge, 2013).
- [36] D. J. Abramovitch, J.-J. Zhou, J. Mravlje, A. Georges, and M. Bernardi, Combining electron-phonon and dynamical mean-field theory calculations of correlated materials: Transport in the correlated metal Sr<sub>2</sub>RuO<sub>4</sub>, *Phys. Rev. Mater.* **7**, 093801 (2023).
- [37] M. Royo, K. R. Hahn, and M. Stengel, Using high multipolar orders to reconstruct the sound velocity in piezoelectrics from lattice dynamics, *Phys. Rev. Lett.* **125**, 217602 (2020).
- [38] A. C. Genz and A. A. Malik, Remarks on algorithm 006: An adaptive algorithm for numerical integration over an N-dimensional rectangular region, *J. Comput. Appl. Math.* **6**, 295 (1980).

- [39] HCubature.jl (v1.5.1), <https://github.com/JuliaMath/HCubature.jl> (2022).
- [40] QuadGK.jl (v2.7.0), <https://github.com/JuliaMath/QuadGK.jl> (2023).
- [41] A. Dal Corso, M. Posternak, R. Resta, and A. Baldereschi, Ab initio study of piezoelectricity and spontaneous polarization in ZnO, *Phys. Rev. B* **50**, 10715 (1994).
- [42] F. Bernardini, V. Fiorentini, and D. Vanderbilt, Spontaneous polarization and piezoelectric constants of III-V nitrides, *Phys. Rev. B* **56**, R10024(R) (1997).
- [43] G. Sági-Szabó, R. E. Cohen, and H. Krakauer, First-principles study of piezoelectricity in PbTiO<sub>3</sub>, *Phys. Rev. Lett.* **80**, 4321 (1998).
- [44] P. Giannozzi, O. Andreussi, T. Brumme, O. Bunau, M. B. Nardelli, M. Calandra, R. Car, C. Cavazzoni, D. Ceresoli, M. Cococcioni, N. Colonna, I. Carnimeo, A. D. Corso, S. de Gironcoli, P. Delugas, R. A. DiStasio, A. Ferretti, A. Floris, G. Fratesi, G. Fugallo *et al.*, Advanced capabilities for materials modelling with Quantum ESPRESSO, *J. Phys.: Condens. Matter* **29**, 465901 (2017).
- [45] X. Gonze, F. Jollet, F. A. Araujo, D. Adams, B. Amadon, T. Applencourt, C. Audouze, J.-M. Beuken, J. Bieder, A. Bokhanchuk, E. Bousquet, F. Bruneval, D. Caliste, M. Côté, F. Dahm, F. D. Pieve, M. Delaveau, M. D. Gennaro, B. Dorado, C. Espejo *et al.*, Recent developments in the ABINIT software package, *Comput. Phys. Commun.* **205**, 106 (2016).
- [46] X. Gonze, B. Amadon, G. Antonius, F. Arnardi, L. Baguet, J.-M. Beuken, J. Bieder, F. Bottin, J. Bouchet, E. Bousquet, N. Brouwer, F. Bruneval, G. Brunin, T. Cavignac, J.-B. Charraud, W. Chen, M. Côté, S. Cottenier, J. Denier, G. Geneste *et al.*, The Abinit project: Impact, environment and recent developments, *Comput. Phys. Commun.* **248**, 107042 (2020).
- [47] D. R. Hamann, Optimized norm-conserving Vanderbilt pseudopotentials, *Phys. Rev. B* **88**, 085117 (2013).
- [48] M. van Setten, M. Giantomassi, E. Bousquet, M. Verstraete, D. Hamann, X. Gonze, and G.-M. Rignanese, The PseudoDojo: Training and grading a 85 element optimized norm-conserving pseudopotential table, *Comput. Phys. Commun.* **226**, 39 (2018).
- [49] J. P. Perdew, K. Burke, and M. Ernzerhof, Generalized gradient approximation made simple, *Phys. Rev. Lett.* **77**, 3865 (1996).
- [50] G. Pizzi, V. Vitale, R. Arita, S. Blügel, F. Freimuth, G. Géranton, M. Gibertini, D. Gresch, C. Johnson, T. Koretsune, J. Ibañez-Azpiroz, H. Lee, J.-M. Lihm, D. Marchand, A. Marrazzo, Y. Mokrousov, J. I. Mustafa, Y. Nohara, Y. Nomura, L. Paulatto *et al.*, Wannier90 as a community code: New features and applications, *J. Phys.: Condens. Matter* **32**, 165902 (2020).
- [51] J. Bezanson, A. Edelman, S. Karpinski, and V. B. Shah, Julia: A fresh approach to numerical computing, *SIAM Rev.* **59**, 65 (2017).
- [52] N. D. Mermin, Lindhard dielectric function in the relaxation-time approximation, *Phys. Rev. B* **1**, 2362 (1970).
- [53] M. Born and K. Huang, *Dynamical Theory of Crystal Lattices* (Oxford University Press, Oxford, 1954).
- [54] J.-J. Zhou, J. Park, I.-T. Lu, I. Maliyov, X. Tong, and M. Bernardi, Perturbo: A software package for ab initio electron-phonon interactions, charge transport and ultrafast dynamics, *Comput. Phys. Commun.* **264**, 107970 (2021).
- [55] R. Resta, Theory of the electric polarization in crystals, *Ferroelectrics* **136**, 51 (1992).
- [56] R. D. King-Smith and D. Vanderbilt, Theory of polarization of crystalline solids, *Phys. Rev. B* **47**, 1651 (1993).
- [57] D. Vanderbilt and R. D. King-Smith, Electric polarization as a bulk quantity and its relation to surface charge, *Phys. Rev. B* **48**, 4442 (1993).
- [58] R. Resta, Macroscopic polarization in crystalline dielectrics: The geometric phase approach, *Rev. Mod. Phys.* **66**, 899 (1994).
- [59] M. Grimsditch, E. S. Zouboulis, and A. Polian, Elastic constants of boron nitride, *J. Appl. Phys.* **76**, 832 (1994).
- [60] X. Gonze and C. Lee, Dynamical matrices, born effective charges, dielectric permittivity tensors, and interatomic force constants from density-functional perturbation theory, *Phys. Rev. B* **55**, 10355 (1997).
- [61] X. Wu, D. Vanderbilt, and D. R. Hamann, Systematic treatment of displacements, strains, and electric fields in density-functional perturbation theory, *Phys. Rev. B* **72**, 035105 (2005).
- [62] H. Lee, S. Poncé, K. Bushick, S. Hajinazar, J. Lafuente-Bartolome, J. Leveillee, C. Lian, J.-M. Lihm, F. Macheda, H. Mori, H. Paudyal, W. H. Sio, S. Tiwari, M. Zacharias, X. Zhang, N. Bonini, E. Kioupakis, E. R. Margine, and F. Giustino, Electron-phonon physics from first principles using the EPW code, *npj Comput. Mater.* **9**, 156 (2023).
- [63] J. Xu, A. Habib, S. Kumar, F. Wu, R. Sundararaman, and Y. Ping, Spin-phonon relaxation from a universal ab initio density-matrix approach, *Nat. Commun.* **11**, 2780 (2020).
- [64] C. Verdi, F. Caruso, and F. Giustino, Origin of the crossover from polarons to Fermi liquids in transition metal oxides, *Nat. Commun.* **8**, 15769 (2017).
- [65] N. Kandolf, C. Verdi, and F. Giustino, Many-body Green's function approaches to the doped Fröhlich solid: Exact solutions and anomalous mass enhancement, *Phys. Rev. B* **105**, 085148 (2022).
- [66] F. Macheda, P. Barone, and F. Mauri, Electron-phonon interaction and longitudinal-transverse phonon splitting in doped semiconductors, *Phys. Rev. Lett.* **129**, 185902 (2022).
- [67] F. Macheda, T. Sohler, P. Barone, and F. Mauri, Electron-phonon interaction and phonon frequencies in two-dimensional doped semiconductors, *Phys. Rev. B* **107**, 094308 (2023).
- [68] I.-T. Lu, J.-J. Zhou, J. Park, and M. Bernardi, First-principles ionized-impurity scattering and charge transport in doped materials, *Phys. Rev. Mater.* **6**, L010801 (2022).
- [69] J. Leveillee, X. Zhang, E. Kioupakis, and F. Giustino, Ab initio calculation of carrier mobility in semiconductors including ionized-impurity scattering, *Phys. Rev. B* **107**, 125207 (2023).
- [70] A. Eiguren, S. de Gironcoli, E. V. Chulkov, P. M. Echenique, and E. Tosatti, Electron-phonon interaction at the Be(0001) surface, *Phys. Rev. Lett.* **91**, 166803 (2003).
- [71] F. Giustino, M. L. Cohen, and S. G. Louie, Small phonon contribution to the photoemission kink in the copper oxide superconductors, *Nature (London)* **452**, 975 (2008).
- [72] Z. Li, M. Wu, Y.-H. Chan, and S. G. Louie, Unmasking the origin of kinks in the photoemission spectra of cuprate superconductors, *Phys. Rev. Lett.* **126**, 146401 (2021).
- [73] J. Noffsinger, E. Kioupakis, C. G. Van de Walle, S. G. Louie, and M. L. Cohen, Phonon-assisted optical absorption in silicon from first principles, *Phys. Rev. Lett.* **108**, 167402 (2012).
- [74] C. E. Patrick and F. Giustino, Unified theory of electron-phonon renormalization and phonon-assisted optical absorption, *J. Phys.: Condens. Matter* **26**, 365503 (2014).

- [75] J.-M. Lihm and C.-H. Park, Wannier function perturbation theory: Localized representation and interpolation of wave function perturbation, *Phys. Rev. X* **11**, 041053 (2021).
- [76] E. R. Margine and F. Giustino, Anisotropic Migdal–Eliashberg theory using Wannier functions, *Phys. Rev. B* **87**, 024505 (2013).
- [77] G. M. Eliashberg, Interactions between electrons and lattice vibrations in a superconductor, *Sov. Phys. JETP* **11**, 696 (1960).
- [78] G. M. Eliashberg, Temperature Green’s function for electrons in a superconductor, *J. Exptl. Theoret. Phys. (U.S.S.R.)* **39**, 1437 (1960) [*Sov. Phys. JETP* **12**, 1000 (1961)].
- [79] J.-J. Zhou and M. Bernardi, Ab initio electron mobility and polar phonon scattering in GaAs, *Phys. Rev. B* **94**, 201201 (2016).
- [80] J. Carrete, W. Li, L. Lindsay, D. A. Broido, L. J. Gallego, and N. Mingo, Physically founded phonon dispersions of few-layer materials and the case of borophene, *Mater. Res. Lett.* **4**, 204 (2016).
- [81] C. Lin, S. Poncé, and N. Marzari, General invariance and equilibrium conditions for lattice dynamics in 1D, 2D, and 3D materials, *npj Comput. Mater.* **8**, 236 (2022).
- [82] B. Pandey and P. B. Littlewood, Going beyond the cumulant approximation: Power series correction to the single-particle Green’s function in the Holstein system, *Phys. Rev. Lett.* **129**, 136401 (2022).
- [83] J. P. Nery, P. B. Allen, G. Antonius, L. Reining, A. Miglio, and X. Gonze, Quasiparticles and phonon satellites in spectral functions of semiconductors and insulators: Cumulants applied to the full first-principles theory and the Fröhlich polaron, *Phys. Rev. B* **97**, 115145 (2018).